Stem Cell Reports
Article

OPEN ACCESS

A Functional Bioluminescent Zebrafish Screen for Enhancing Hematopoietic Cell Homing

Yuliana Astuti,[1] Ashley C. Kramer,[1] Amanda L. Blake,[1] Bruce R. Blazar,[1] Jakub Tolar,[1] Mandy E. Taisto,[1] and Troy C. Lund[1,*]

[1]Department of Pediatrics, Blood and Marrow Transplant Program, University of Minnesota Medical School, MMC 366, 420 Delaware Street Southeast, Minneapolis, MN 55455, USA

*Correspondence: lundx072@umn.edu

http://dx.doi.org/10.1016/j.stemcr.2016.12.004

SUMMARY

To discover small molecules that modulate hematopoietic cell homing after adoptive transfer, we created a transgenic zebrafish expressing firefly luciferase downstream of the *ubiquitin* promoter (*ubi:luc*) to serve as a hematopoietic donor. Bioluminescence imaging (BLI) was used to detect and follow *ubi:luc* hematopoietic cells that homed to the marrow as early as 1 day post-transplant. BLI was able to detect the biological effect of prostaglandin E_2 on early homing/engraftment of donor hematopoietic cells. This system was utilized in a functional screen of small molecules to enhance homing/engraftment. We discovered a phytosterol, ergosterol, that could increase hematopoietic cell homing in zebrafish and mice. In addition, ergosterol increased CXCR4 expression and promoted expansion of $Lin^-SCA\text{-}1^+KIT^+$ cells in vitro. We have demonstrated the utility of in vivo BLI to non-invasively monitor donor hematopoietic cell activity in adult zebrafish as a functional screen for mediators of cellular homing.

INTRODUCTION

The zebrafish is a useful organism to model hematopoietic cell transplantation (HCT). As in mammals, transplanted zebrafish hematopoietic stem/progenitor cells (HSPC) collected from whole kidney marrow (WKM) are able to repopulate all hematopoietic lineages and provide long-term reconstitution in irradiated recipient fish (Traver et al., 2004). Furthermore, many of the biological aspects important for successful HCT in mammals are conserved in zebrafish. Two recent examples include the role of major histocompatibility complex matching and our prior work demonstrating the role of *stromal derived factor-1* (SDF-1) in HSPC homing activity (de Jong et al., 2011; Glass et al., 2011, 2013).

Cellular engraftment in adult zebrafish is determined by analyzing the WKM of the recipients, typically by measuring the fluorophore-labeled donor cells using flow cytometry. With the development of transparent Casper fish (White et al., 2008), the fluorescent hematopoietic cells from the donor can also be monitored in vivo via live imaging, which could provide a more complete picture of the hematopoietic recovery process after transplant. However, despite its rapid acquisition time and high resolution, the sensitivity of fluorescent imaging can be severely reduced by high background noise and limited tissue penetration, preventing the detection of low signals in deep tissue, such as those during hematopoietic cell homing and early engraftment in the kidney within the first few days after HCT. Bioluminescence imaging (BLI), on the other hand, has an excellent signal-to-noise ratio, as there is virtually no background in the tissues (Lin et al., 2008). In murine HCT, donor cell tracking by non-invasive BLI can reveal the dynamics of different hematopoietic cell repopulation in the recipients (Cao et al., 2004; Wang et al., 2003). Although in mice, robust BLI is generated 7–8 days post-HCT, the optical clarity of the zebrafish is ideal for the development of BLI to track hematopoietic cell homing function within the first few days after HCT.

To explore the suitability of BLI for tracking the transplanted donor hematopoietic cells, we generated *ubi:luc* zebrafish that ubiquitously expressed firefly luciferase under control of the *luciferase* promoter and used this transgenic line as a WKM donor in HCT. We showed that, using BLI, luciferase-expressing donor hematopoietic cells could be continuously monitored in the same individual to demonstrate the kinetics of the hematopoietic reconstitution following transplantation in adult zebrafish. Furthermore, we demonstrate that this BLI-based system has use as a "functional" chemical screen of small molecules that enhance homing and engraftment.

RESULTS

Luciferase Expression in *ubi:luc* Hematopoietic Cells

To produce a transgenic hematopoietic cell donor suitable for BLI, we cloned a 3.5-kb fragment of the zebrafish *ubiquitin* gene (*ubi*) upstream of firefly (*Photinus pyralis*) *luciferase* on a Tol2 backbone that also contained a cardiac myosin light-chain promoter-driven EGFP to allow rapid identification of transgenic animals. Previously, this fragment was shown to be sufficient to drive expression in nearly all zebrafish tissues at multiple stages of

This is an open access article under the CC BY-NC-ND license (http://creativecommons.org/licenses/by-nc-nd/4.0/).

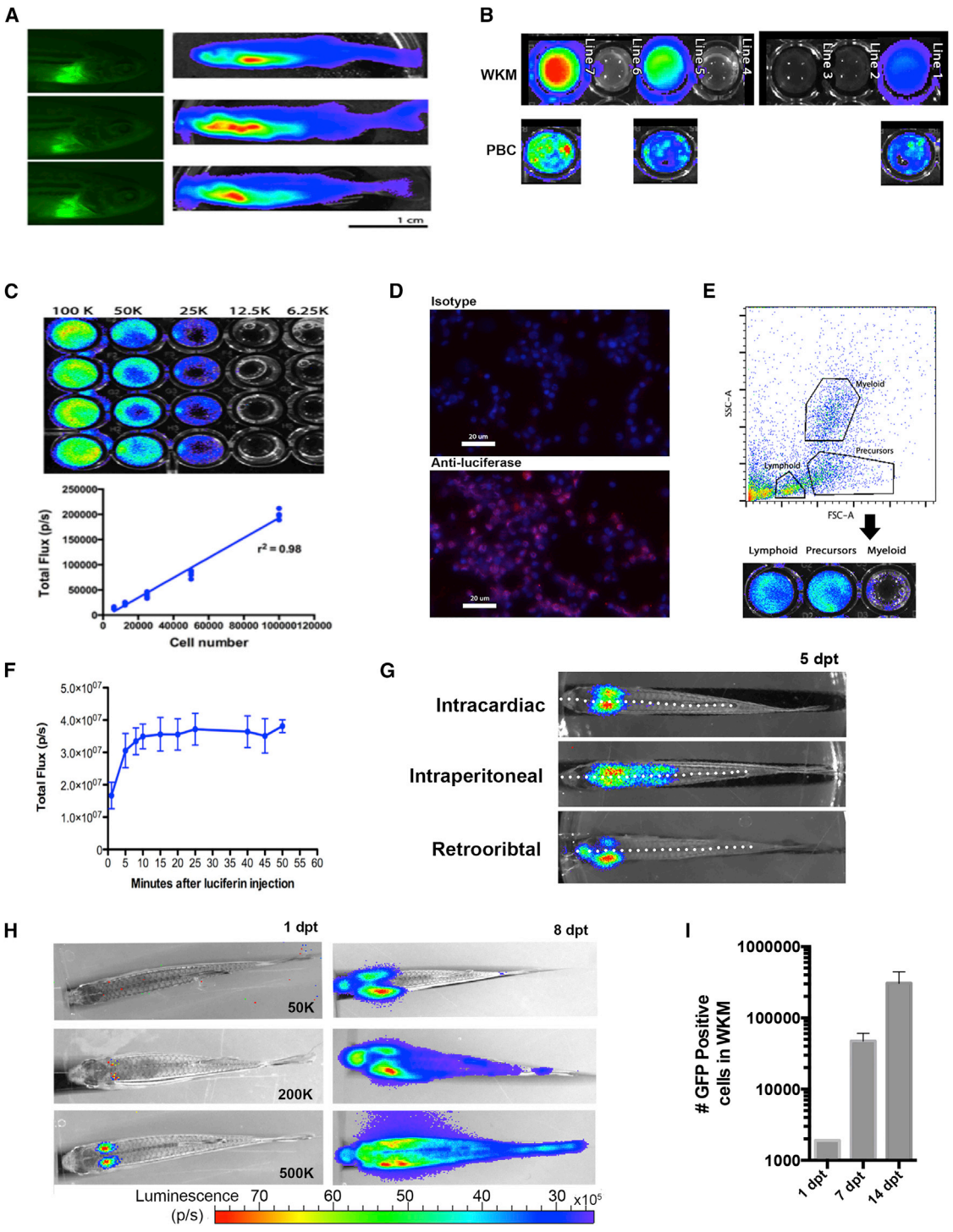

Figure 1. Luciferase Expression in *ubi:luc* Zebrafish

(A) Adult founder zebrafish with EGFP fluorescent hearts (*cmlc:EGPF*) derived from the Tol2 backbone. Whole-body BLI visualized after intraperitoneal injection of D-luciferin. Three of 20 potential founder lines are shown.

(B) WKM correlates with PBC BLI from three F2 fish lines.

(C) Limiting dilution of WKM from *ubi:luc* indicates a linear BLI signal with detection to 6,250 cells in vitro. Data shown are mean ± SD and r^2 from Pearson's correlation (n = 6 wells per cell concentration).

(legend continued on next page)

development (Mosimann et al., 2011). Founder transgenic embryos were screened by the application of D-luciferin to the embryo water (Figure S1A). Founders were outbred to obtain germline F1 animals (screened by BLI as embryos) that subsequently were outbred to produce F2 offspring. Many adult F2 animals displayed high levels of total-body BLI as shown in Figure 1A but, upon dissection of various organs from F2 adults, we found that individual animals had a mixture of organs with a strong BLI signal as well as some without a signal (Figure S1B). We identified three F1 lines to propagate F2 animals with high levels of WKM BLI (Figure 1B). WKM correlated very well with peripheral blood BLI allowing future adult screening to be performed by obtaining peripheral blood from a tail vein. Line 7 gave a robust WKM BLI signal, and clutch offspring produced a WKM BLI intensity that varied by less than 10% in most cases (therefore, this line was used for most downstream experiments) (Figure 1C). Serial dilution of WKM in vitro showed a high degree of linear correlation between cell number and BLI signal (r^2 = 0.98, Figure 1C). When the charge-coupled device (CCD) resolution was increased to 8-pixel binning, BLI could be detected in as low as 6,250 cells (Figure S1C). Immunostaining of WKM showed that the majority of WKM expressed luciferase (Figure 1D). To examine if *ubi:luc* was expressed by specific blood cell lineages, WKM cells were sorted into lymphoid, myeloid, and the progenitor-enriched precursor subpopulations with fluorescence-activated cell sorting (Traver et al., 2003). Following substrate addition, a bioluminescent signal was detected in all three blood cell populations (Figure 1E), although somewhat attenuated in the myeloid population, which we speculate may be due to promoter function downregulation.

Optimizing BLI for Homing of Hematopoietic Cells

We initially attempted to either bathe *ubi:luc* zebrafish in D-luciferin (150 μg/mL) or use intraperitoneal injection (75 μg) and found intraperitoneal injection was significantly more robust in producing BLI in our system (Figure S1D). Note that our bathing dose of D-luciferin (0.5 mM) was considerably lower than other reports that used 50–100 mM for a bathing technique (Chen et al., 2013). Therefore, further studies used an intraperitoneal injection of D-luciferin. To determine the optimal timing for luminescence image acquisition after HCT, we followed the time course of light emission after D-luciferin administration in adult transplant recipients for 55 min. Five animals were given an intraperitoneal injection of D-luciferin (75 μg), followed by serial imaging every 2–5 min. The luminescent signal increased gradually until it reached a plateau phase at 10 min and remained relatively stable for the remaining 45 min, which was nearly identical to that reported by Chen et al. (2013) using a similar model (Figure 1F). Despite the long plateau period with this dose of D-luciferin, we standardized the acquisition time to a maximum of 15 min after the injection to minimize variability. We next assessed intracardiac, intraperitoneal, and retro orbital injection routes for HCT cell delivery (Figure 1G). Intraperitoneal injection produced a robust homing/engraftment BLI signal at 1 and 5 days post-transplant (dpt), although 50%–80% of the animals died within 5 days of HCT. Retro orbital injection also achieved a robust BLI signal, but homing/engraftment BLI was often asymmetric (higher on the injected side of the body), probably due to the unilateral cell dose delivery. Intracardiac delivery gave robust, symmetrical, and consistent WKM homing/engraftment BLI and therefore was used in all future experiments. We next assessed the numbers of donor WKM cells needed to visualize homing 1 day post-transplant. Figure 1H shows that between 200,000 and 500,000 donor *ubi:luc* cells gave rise to robust signal symmetrically distributed in the WKM (Figure 1H). HCT of 50,000 cells could produce BLI signal from engrafting WKM at 8 dpt, but earlier imaging did not always result in a consistent signal. In addition, we found improved 28-day survival with 200,000 donor WKM cells (Figure S1E). Using 500,000

(D) Immunostaining of cytopspun *ubi:luc* WKM cells showing luciferase expression cells. Anti-mouse IgG1-Cy3 secondary antibody was used for detection and DAPI was used as a nuclear stain.
(E) Zebrafish WKM from *ubi:luc* was sorted by flow cytometry into lymphoid, precursor, and myeloid subpopulations based on forward- and side-scatter gating followed by BLI in a 96-well plate.
(F) Zebrafish received 20 Gy radiation, underwent HCT with 500,000 *ubi:luc donor cells*, and were allowed to engraft for 28 days. To determine an optimal time for BLI acquisition, recipient fish were injected with 5 μL of 15 mg/mL D-luciferin in PBS and then serially imaged on an IVIS imaging system. Data shown are mean ± SD (n = 5 individual zebrafish).
(G) Examples of WKM engraftment after three injection routes. A total of 200,000 *ubi:luc* WKM cells was delivered 2 days after recipients received 20 Gy X-ray radiation. BLI was performed at 5 days post-transplant (dpt). The dotted white lines represent the mid-line of the fish body.
(H) *ubi:luc* WKM can be detected at 1 dpt. Animals underwent HCT with the indicated number of WKM cells delivered via intracardiac injection.
(I) Rapid expansion of *ubi:luc* x *h2afv:GFP* donor WKM. HCT was performed with 200,000 donors cells. WKM was harvested at the given time points, and GFP donor cells enumerated by flow cytometry. Shown are mean ± SD (n = 6 individual zebrafish).
See also Figure S1.

donor WKM cells produced a signal we deemed to be robust enough to use as a baseline; therefore, for downstream experiments, a dose of 200,000 donor WKM cells was chosen as the dose for future HCT. To confirm that the BLI signal was being emitted from donor cells homed to the head kidney, we performed HCT using donor WKM from *ubi:luc* crossed to *h2afv*:GFP (*h2afv* is a ubiquitous promoter), which expresses a robust GFP signal in all tissue types including hematopoietic cells (Pauls et al., 2001). The recipient WKM was harvested at 1 dpt and flow cytometry was used to quantify numbers of donor cells homed. The mean number of WKM cells homed at 1 dpt was 1,897 ± 33 cells, very similar to the minimum number of WKM cells required for engraftment reported by de Jong et al. (2011). Following homing, rapid expansion was seen, with a mean of 47,263 ± 13,662 cells and 306,459 ± 136,561 cells engrafted at 7 and 14 dpt, respectively (Figure 1I).

While our priority was to use the *ubi:luc* model to investigate homing within 24–48 hr of HCT, being able to consistently assess long-term evaluation of HCT would be also useful. Our initial experiments with BLI after HCT, using 200,000 donor cells and animals undergoing sedated BLI acquisition at 1 and 5 dpt, showed poor survival (100% deaths by 10 days post-HCT) (Figure S1F). Typical survival at 30 days post-HCT with 200,000 donor cells without BLI is approximately 50% as shown in our control experiments, and is also in agreement with that reported by de Jong et al. (2011). We reasoned that the low survival might be due to overwhelming stress and hypoxia on the animals during BLI. Therefore, we modified sedation conditions to include hyperoxgenated fish water to provide a source of oxygen during periods of low oxygen exchange during sedation, which allowed for equivalent survival to transplanted animals not undergoing sedated BLI and was used in the later experiments (Figure S1F). Together, these data show that, under optimum conditions, BLI can be used to assess early hematopoietic cell homing in the zebrafish.

Longitudinal Detection of Donor Cells Following Transplantation

We studied the dynamics of hematopoietic cell homing and engraftment in adult zebrafish by performing BLI on recipient fish, at multiple time points, on both radiation-conditioned and non-irradiated recipients transplanted with 500,000 *ubi:luc* WKM cells. At 1 dpt the luminescent signal was detectable in the head kidney (the site of robust hematopoiesis) in both radiated and non-irradiated recipients, although there was less signal in the absence of radiation (Figure 2A). This indicated that, similar to what has been shown in mice, the migration of donor hematopoietic cells to the marrow does not require radiation preconditioning of the host. Robust and accumulative signal was observed in 20-Gy-irradiated recipients over time, while donor cells were not detected in non-irradiated recipients by 7 dpt (even as early as 2 dpt). The signal in irradiated recipients continued to increase until 4 weeks post-transplant, after which it decreased to a lower, more steady level of luminescence that was maintained for at least 3 months after transplant (Figure 2B). These studies confirm that homing occurs in the absence of radiation conditioning (as also observed in murine experiments), but rejection ensues, and long-term engraftment does not occur, likely due to innate and/or adaptive immune responses. Further experiments to fine-tune the dose of radiation (15 versus 20 Gy) showed that there was a slight, but not significant, increase in donor hematopoietic cell BLI at 1 and 8 dpt using 20 Gy, which was ultimately chosen for screening experiments (Figures S2A and S2B).

To test the ability of a small molecule to modulate homing in our system we used dimethyl prostaglandin E_2 ($dmPGE_2$), which has been previously characterized to modulate HSPC homing, engraftment, and HSPC survival in zebrafish, mice, and human studies (Hoggatt et al., 2009; North et al., 2007; Porter et al., 2013). We treated 200,000 *ubi:luc* WKM cells with 10 μM $dmPGE_2$ for 2 hr on ice prior to HCT. We found a significantly higher rate of cellular homing at 1 dpt, as well as improved early engraftment (at 7 dpt), similar to published murine studies (Frisch et al., 2009) (Figures 2C and 2D). Later engraftment was similar to controls (14 dpt and beyond). The early homing/engraftment correlated well with increased survival after HCT (Figure 2E). In this system, $dmPGE_2$ accelerated early hematopoietic cell recovery, but no differences were seen at 14 dpt or later, most likely because control animals engrafted slower, but the animals that survived did ultimately engraft to the same extent as the $dmPGE_2$-treated group. These experiments indicated that BLI using *ubi:luc* donor WKM is a valid and robust platform on which to perform small-molecule screening for enhancers of HCT homing (Figure S2C).

Screening for Enhancement of Hematopoietic Cell Homing

We performed HCT using *ubi:luc* WKM treated with 10 μM of candidate compound from a library of naturally occurring compounds with known biologic activity (n = 860), but that have not been explored in the modulation of hematopoietic cell homing. We could easily transplant 50–100 animals in a single day. Assessment of homed hematopoietic cells was determined by BLI at 1 dpt. Each experiment had control HCT recipients (using DMSO-treated donor WKM) performed in triplicate. An example of the first screen of the chemical library is shown in Figure 2F. We found 78 candidate "hits" in this first screen,

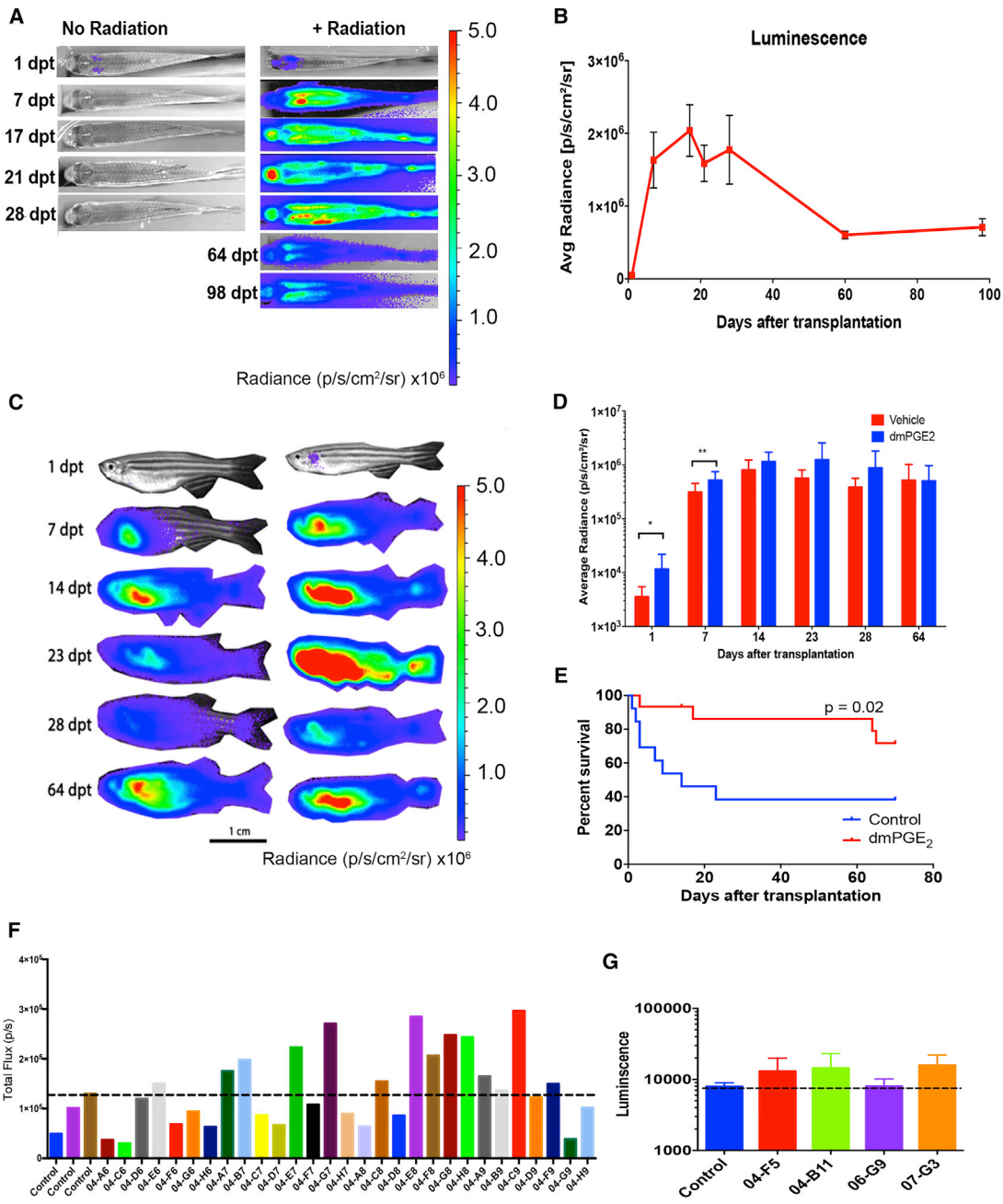

Figure 2. Small-Molecule Screening to Enhance Homing of Donor Cells

(A) Serial BLI of non-irradiated and 20-Gy-irradiated recipients receiving 500,000 *ubi:luc* WKM cells.

(B) Average ± SD radiance of engrafted recipients over time, n = 6 individuals/group.

(C) Serial BLI of recipients transplanted with vehicle- and dmPGE$_2$-treated *ubi:luc* WKM cells.

(D) BLI quantification of recipients in vehicle- and dmPGE$_2$-treated groups, n = 13 individuals/group, data shown are mean ± SD, *p < 0.05, **p < 0.01, from a Student's t test.

(E) Survival of recipients from control and dmPGE$_2$-treated groups is significantly different, n = 13 individuals/group.

(F) Example of the BLI readout from a series of tested compounds. All recipients received 200,000 *ubi:luc* donor cells co-incubated with 10 μM of compound prior to HCT. Each bar represents one animal. The dashed line shows the highest BLI in one of three control animals for that experimental group.

(G) Second screen of initial hits with n = 3–5 animals per compound. Data show a dashed line at the control mean ± SD. This example shows compound 04-B11 (ergosterol) that was examined in follow-up studies.

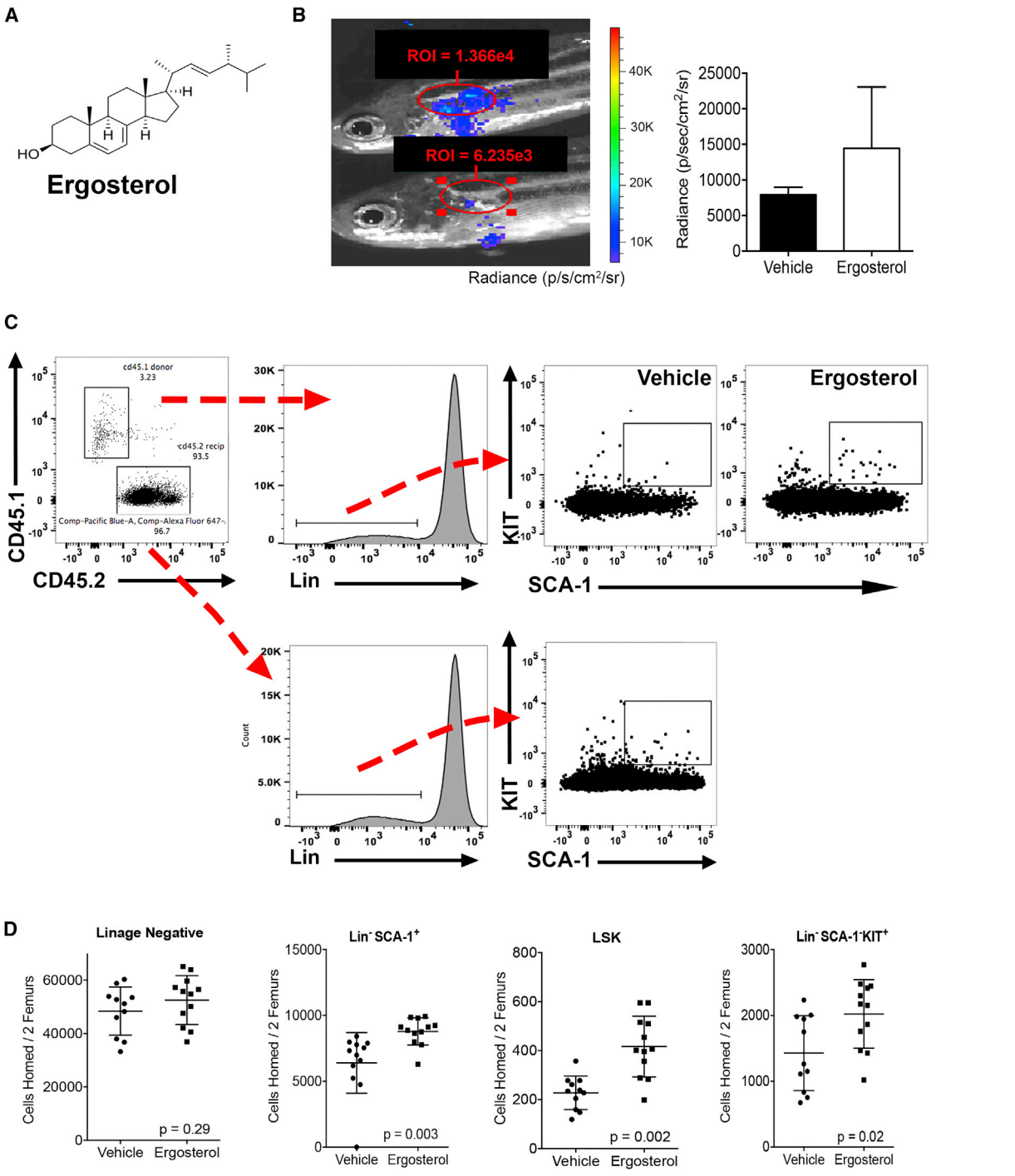

Figure 3. Ergosterol Enhances Murine Hematopoietic Cell Homing

(A) Structure of ergosterol, a member of the sterol family of compounds.

(B) BLI at 1 dpt of fish receiving ergosterol-treated cells in the secondary screen. The region of Interest (ROI) and donor cell radiance values of the WKM are shown. Some residual signal can be seen at the injection site. Right panel shows difference in radiance between vehicle and ergosterol-treated homed donor cells. Data shown are mean ± SD from five individual recipients.

(C) Flow cytometry gating for the identification of $Lin^{-}SCA\text{-}1^{+}KIT^{+}$ donor cells after murine HCT. Initial gates were used to identify mononuclear cells that were propidium iodide (PI) negative.

(legend continued on next page)

with a "hit" being defined as a >25% increase in marrow-homed cells. Hits were subject to a second round of HCT using three to five animals per group, and from this second screen 30 compounds were verified to increased hematopoietic cell homing (examples shown in Figure 2G). At this point, we selected one compound (04-B11), ergosterol, to further evaluate.

Ergosterol Increases Hematopoietic Cell Homing

Ergosterol is a phytosterol (Figure 3A) produced by fungi and mushrooms as part of the cell wall. Interestingly, UV radiation exposure converts ergosterol into ergocalciferol, which is vitamin D_2 (Bikle, 2014). Figure 3B shows an example of ergosterol-mediated increase in homing of *ubi:luc* donor hematopoietic cells 1 dpt. To test for biologic activity in mammalian cells, we increased the ergosterol concentration to 50 μM prior to mixing with donor marrow and at HCT. The rationale for 5-fold increase in compound exposure was due to the fact that, in the zebrafish model, the compound and donor cells were injected into the recipient animals in a 5-μL volume; injection into 10–20 μL of total blood volume gives a circulating concentration of 2–3 μM of compound from a 10 μM stock). The average blood volume of an adult mouse being approximately 1 mL, we reasoned that adding 50 μM of ergosterol in a 0.2-mL injection volume would allow exposure to 10 μM of circulating compound and approximate our zebrafish compound screen platform. Ergosterol or equal v/v treated whole bone marrow (WBM) were injected into lethally irradiated recipient mice. Marrow was harvested 16 hr later and homed donor cells were evaluated by flow cytometry. Unlike zebrafish, more specific murine progenitor cells can be quantified by assessing $Lin^-SCA\text{-}1^+KIT^+$ (LSK) cells that are enriched for hematopoietic stem cell activity (Figures 3C and 3D). The control animals had 228 ± 68 homed LSK cells after HCT, while the ergosterol-treated group had 417 ± 124 homed LSK cells ($p = 0.002$, $n = 10$) (Figure 3D). We also found a significant increase in homed $Lin^-SCA\text{-}1^+$ cells ($p = 0.003$, Figure 3D), but not in lineage-negative cells ($p = 0.29$, Figure 3D). $Lin^-SCA\text{-}1^-KIT^+$ cells also showed a homing advantage in the ergosterol-treated group ($p = 0.02$); this cell population often contains granulocyte macrophage progenitor, common myeloid progenitor, and megakaryocyte erythrocyte progenitor subpopulations.

Ergosterol Increases CXCR4

Because our platform relies on delivering compounds and hematopoietic cells to the recipient animals, one can argue that there are effects on the recipient microenvironment to make it more favorable for homing as well as effects on the donor hematopoietic cells. Given the complex nature and cellular makeup of the niche microenvironment, we chose initially to better understand the effects of ergosterol on the donor hematopoietic cells.

We performed in vitro cell migration assays as depicted in Figure 4A. Murine WBM cells were assessed for their ability to migrate toward an SDF-1 gradient in the presence of ergosterol. This, and subsequent assays, utilized 10 μM ergosterol as that was the approximate circulating concentration in the murine homing experiments. Ergosterol-treated murine bone marrow cells showed a significantly greater migration toward SDF-1 than controls ($p < 0.001$, Figure 4B). One of the most well-studied receptors governing hematopoietic cell migration is CXCR4, a primary receptor for SDF-1 (Peled et al., 1999). There are several reports that vitamin D family members are very effective at upregulating CXCR4 expression on hematopoietic cells (Biswas et al., 1998; Hiraguchi et al., 2012; Savli et al., 2002). In agreement with these reports, we found that murine bone marrow mononuclear cells exposed to ergosterol for 12 hr increased *Cxcr4* gene expression by greater than 1.5-fold (Figure 4C). Flow cytometry of similarly treated WBM cells revealed that approximately 2-fold more lineage-negative cells expressed CXCR4 on the cell surface (Figure 4D) and CXCXR4 mean fluorescence intensity also increased 2-fold ($p < 0.0001$, Figure 4E). Lin^-Sca1^+ and LSK also demonstrated significantly increased CXCR4 expression after ergosterol exposure ($p < 0.0001$, Figures 4F and 4G). These data are consistent with the hypothesis that CXCR4 modulation may contribute to the biologic activity of ergosterol related to homing.

Vitamin D response elements (VDRE) are prevalent throughout the genome (Carlberg, 2003), and we next sought to determine if ergosterol, a vitamin D family member, could activate VDRE as a potential mechanism of action. We utilized a reporter system in which VDRE regulates luciferase to test this hypothesis. VDRE-reporting HEK293 cells showed no VDRE activity after 12 hr of ergosterol exposure compared with vehicle control, while calcitriol (1,25-dihydroxyvitamin D_3) stimulated VDRE activity as expected (Figures 4H and 4I). To ascertain whether the vitamin D receptor (VDR) could enhance VDRE activity in the presence of ergosterol, we transiently transfected VDRE-reporting HEK293 cells with a copy of the murine *Vdr* gene (NM_0095494). While the expression of the VDR enhanced calcitriol-mediated VDRE signaling by

(D) Ten million CD45.1 donor cells in 50 μM ergosterol (circulating concentration estimated at 10 μM) or equal v/v vehicle were transplanted into CD45.2 lethally irradiated recipients. Bilateral femur marrow was harvested from recipients 16 hr post-transplant. Flow cytometry was used to quantify absolute numbers of homed donor cells using the gating strategy in (C). Data shown are mean ± SD and p values from a Student's t test (n = 10–11 animals/group in two pooled experiments).

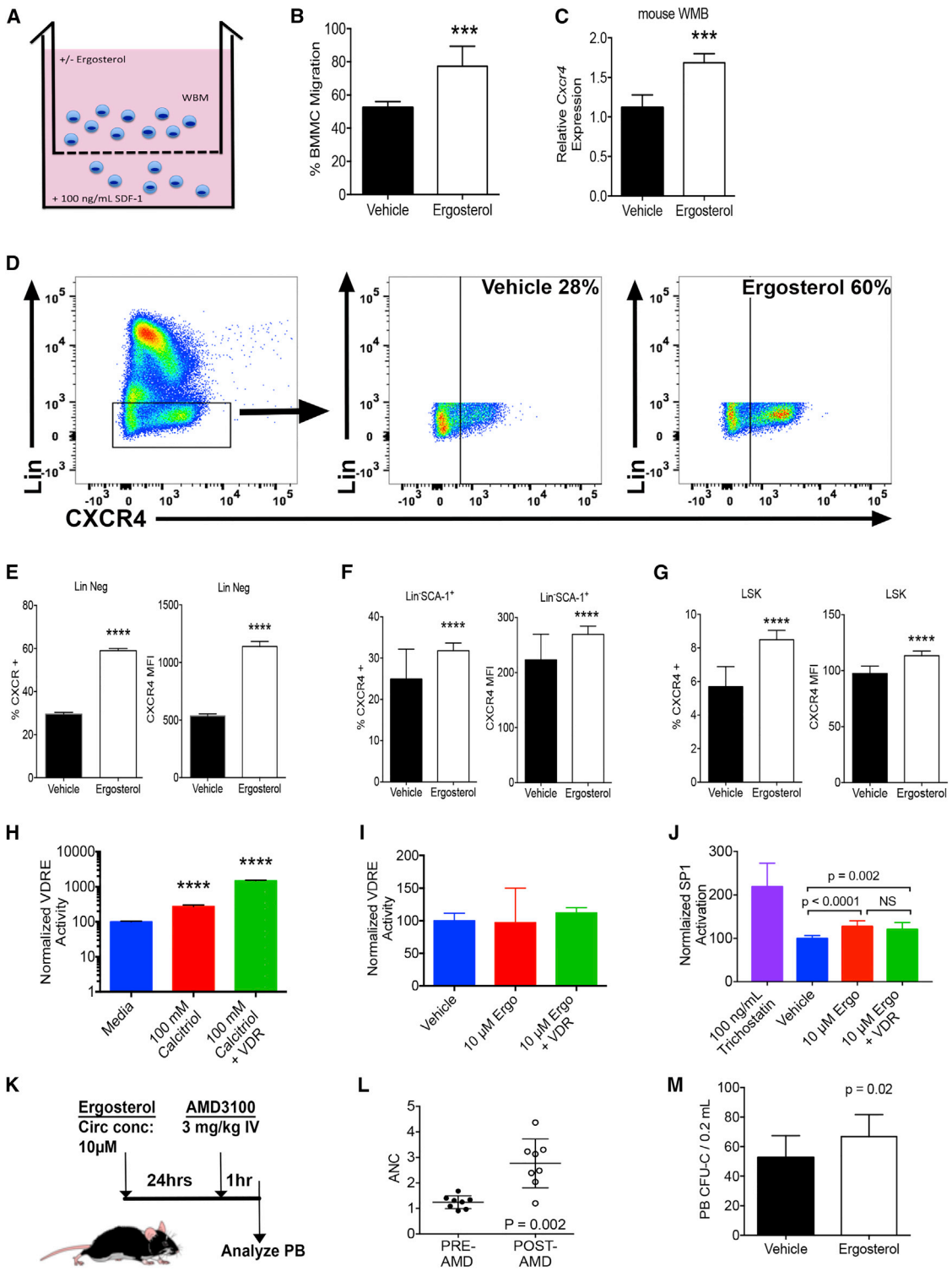

Figure 4. Ergosterol Enhances Hematopoietic Cell Homing via CXCR4

(A) System for testing in vitro migration of murine WBM.

(B) In vitro migration of murine WBM treated with ergosterol versus vehicle. WBM cells were placed in a 3-μm Transwell in the presence of 10 μM ergosterol (or equal v/v of vehicle) and allowed to migrate toward 100 ng/mL rSDF1 overnight. Migrated bone marrow mononuclear cells (BMMC) in the lower chamber were enumerated by flow cytometry (n = 12 wells per group, repeated in triplicate).

(legend continued on next page)

540% (mean luciferase activity 286 versus 1,486, both relative to control, $p < 0.0001$), there was no increase in ergosterol-mediated VDRE signaling (Figures 4H and 4I).

Previous work has shown that the *CXCR4* promoter contains specific protein 1 (SP1) binding elements that activate transcription specifically in the presence of growth factors such as vascular endothelial growth factor, basic fibroblastic growth factor, as well as PGE_2 (Salcedo et al., 2003). We evaluated the ability of ergosterol to increase SP1 activity using an SP1-reporting luciferase-based system (in this assay, the SP1 reporter was transiently transfected). We found that SP1-reporting HEK293 cells exposed to ergosterol showed a 28% increase in SP1 activity compared with vehicle (luciferase activity of 128 versus 100, $p < 0.0001$). SP1 activity was not increased when we expressed the murine VDR with ergosterol exposure (Figure 4J). These data show that ergosterol mediates SP1 activity but not VDRE activity. In both cases, ergosterol seems to function in a VDR-independent manner.

To determine whether an ergosterol-mediated increase in CXCR4 expression could affect functional activity, we utilized AMD3100, a CXCR4 antagonist, to mobilize progenitors from the marrow to the peripheral circulation, as described previously (Ramirez et al., 2009). Mice were injected with ergosterol (to achieve a circulating concentration of 10 μM) 24 hr prior to receiving AMD3100 (3 mg/kg intravenously [i.v.]). We demonstrated that AMD3100 increased the peripheral neutrophil count in mice 1 hr after injection (Figure 4L), although there was no difference in neutrophil mobilization between ergosterol-treated and untreated animals (data not shown). On the contrary, peripheral blood progenitors were assessed using a colony-forming unit - cells (CFU-C) assay and found to be significantly greater in mice that received ergosterol ($p = 0.02$, Figure 4M). These data show that ergosterol-enhanced CXCR4 can potentiate the mobilizing effects of a CXCR4 antagonist, AMD3100.

Ergosterol Improves Cell Viability

To determine if ergosterol had a wider range of biologic effects apart from cell migration, we culture-expanded murine LSK cells in the presence of ergosterol. We found that, after 14 days in culture, ergosterol treatment resulted in a >250% increase in cell numbers over vehicle-alone-treated LSK (Figure 5A). In addition, expanded cells exposed to ergosterol had improved viability after 4 and 14 days in culture (Figure 5B). Given these data on improved hematopoietic cell viability, we tested whether ergosterol could hasten autologous recovery after radiation in the zebrafish model, which would depend on both hematopoietic cell survival and growth/recovery. We exposed zebrafish to 20 Gy X-ray irradiation and allowed them to recover with ergosterol added to water for 14 days. In this experiment, ergosterol was added empirically at 50 μM due to the fact that animals would take up ergosterol through oral- or gill-mediated routes, and the amount taken up would be mostly unknown. Marrow was harvested and assessed by flow cytometry after 14 days (Figures 5C–5E). We found that ergosterol had a significant impact on the recovery of the "precursor" population ($p = 0.002$) as well as increasing the overall cellular viability of the WKM ($p = 0.02$, Figures 5F–5J). These data show that ergosterol can have positive effects on hematopoietic cell expansion as well as viability, suggesting that it has more pleiotropic properties other than increasing CXCR4.

DISCUSSION

The ability to perform HCT in zebrafish has expanded our ability to study vertebrate HSPC and transplant biology.

(C) RT-PCR of murine WBM cells treated for 12 hr with 10 μM ergosterol or vehicle (n = 8 technical replicates per group, data represent one of three independent experiments).
(D) Flow cytometry gating for the identification of CXCR4 expression on murine lineage-negative cells. Initial gates were used to identify mononuclear cells that were PI negative. See also Figure S3.
(E–G) Murine WBM treated for 12 hr with 10 μM ergosterol or equal v/v vehicle followed by flow cytometry for CXCR4 and lineage cocktail as in (D) For $Lin^-SCA\text{-}1^+$ and LSK the flow cytometry gating of Figure 3C was used (n = 8 individual animals from two pooled experiments).
(H and I) HEK293 cells containing the VDRE reporter (luc) were incubated with calcitriol, ergosterol, or equal v/v vehicle followed by the measurement of luciferase. Data were normalized to medium or vehicle sample. In some groups, the murine *Vdr* was transfected into cells 24 hr prior to compound exposure (n = 8 wells per group, representing one of three independent experiments).
(J) HEK293 cells containing the SP1 reporter (luc) were incubated with trichostatin, ergosterol, or equal v/v vehicle followed by the measurement of luciferase. Data were normalized to *Renilla* luciferase and the vehicle-treated samples. In some groups, the murine VDR was transfected into cells 48 hr prior to compound exposure (n = 12 per group from three independent experiments).
(K) Ergosterol enhances AMD3100-mediated progenitor mobilization. Mice were given 0.2 mL of 50 μM ergosterol or equal v/v vehicle (to achieve a circulating concentration of 10 μM) 24 hr prior to AMD3100, delivered at 3 mg/kg i.v. One hour later, mice were euthanized to measure CFU-C in the peripheral blood (PB).
(L) Absolute neutrophil count (ANC) pre- and post-AMD3100.
(M) PB CFU-C of ergosterol-treated mice (n = 8 individual animals from two pooled experiments).
Data shown are mean ± SD and p values from a Student's t test. ****$p < 0.0001$, ***$p < 0.001$; NS not significant.

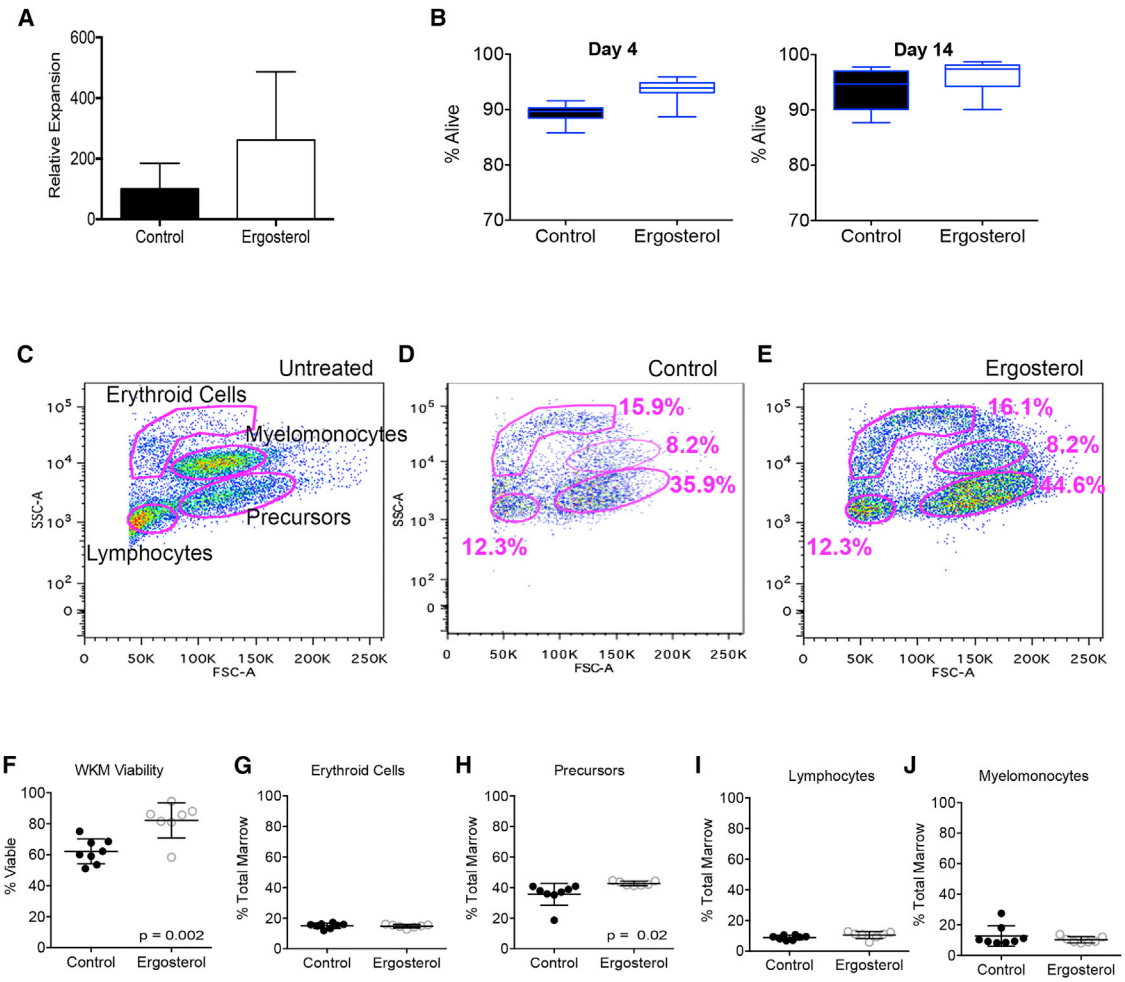

Figure 5. Ergosterol Expands Hematopoietic Progenitors In Vitro, Improves Viability, and Facilitates Radiation Recovery

(A) Murine LSK were plated at 2,500 cells/well in a volume of 400 μL in a 24-well plate (n = 12 wells per group representing one of two experiments). Ergosterol was added at 10 μM (or equal v/v of vehicle). Fresh medium (200 μL) was added every 6 days. Cells were enumerated by flow cytometry after 14 days. Data shown are relative expansion to the control group.

(B) Viability of murine LSK cells after 4 or 14 days in culture days was determined by PI exclusion. Boxplots show the 25th to 75th percentiles with a line at the median, and whiskers represent minimum and maximum values (n = 12 wells per group representing one of two experiments).

(C) Radiation recovery experiment. Zebrafish received 25 Gy irradiation. Twenty-four hours later, 50 μM ergosterol (or equal v/v vehicle) was added to the water. WKM was harvested 14 days after radiation treatment and analyzed by flow cytometry using typical forward- and side-scatter gating for erythroid cells, myelomonocytes, precursors, and lymphocytes, as shown.

(D and E) Representative flow cytometry plots from an animal in the control and ergosterol-treated groups, respectively.

(F) Viability of WKM after autologous recovery determined by PI exclusion in WKM.

(G–J) Recuperation of each cell type after autologous hematopoietic recovery.

All data shown are mean ± SD and p values from Student's t test, unless otherwise noted.

In vivo optical imaging, in contrast to post-mortem analysis of donor cell engraftment, can non-invasively analyze temporal-spatial information of the transplanted hematopoietic cells over time. Unlike fluorescence-based screens, biological tissues do not have inherent bioluminescence giving BLI the advantage of a high signal-to-noise ratio. Furthermore, the wavelength of the light emitted from firefly luciferase-expressing cells is sufficient to produce good tissue penetration in small animals. BLI can be performed with short exposure times allowing a greater number of animals to undergo image acquisition simultaneously and increase throughput. The sensitivity of BLI can be further increased when the transparent adult zebrafish, Casper (derived from mating *roy* and *nacre* pigment

mutants), are used as their light absorption is minimal (White et al., 2008). BLI, being a rapid and sensitive quantitative technique, can facilitate a variety of medium-throughput screens and will be particularly advantageous to use with zebrafish, which is a logistically and financially attractive model for drug discovery.

Our system is very similar to that developed by the Poss Lab using the same ubiquitin promoter fragment (Chen et al., 2013), although their study did not use sedation routinely for BLI acquisition and allowed animals to swim freely (donor BLI was assessed 28 days post-HCT). By optimizing sedation and keeping the animals immobile, we were able to measure the fraction of hematopoietic cells that homed to the WKM 24 hr post-HCT, a unique feature of our approach. BLI-based studies in mice using luciferase-expressing donor cells can also measure homed cells as early as 24 hr post-HCT, but the spatial-temporal location of the migrated cells is not as precise as the studies we have performed (Wang et al., 2003).

In our first screen, we identified a compound, ergosterol, as a positive mediator of hematopoietic cell homing in zebrafish and mice. Ergosterol is a sterol family member produced by mushrooms and fungi in significant quantities. After UVB irradiation, ergosterol is converted to vitamin D_2 (ergocalciferol), which is a vitamin D analog. Unlike vitamin D_3, D_2 is not readily converted into 25 hydroxyvitamin D, the precursor to the active form of vitamin D, $1,25(OH)_2D_3$. While historical data suggest that vitamin D_2 does bind to the VDR with a similar affinity as vitamin D_3 metabolites, vitamin D_2 has less vitamin D binding protein affinity, shortening its plasma half-life, and it has been suggested that it is not equivalent to vitamin D_3 in potency (Hollis, 1984; Houghton and Vieth, 2006). Our data indicating that ergosterol does not act through VDR also suggest an alternative to the classic vitamin D_3-VDR pathway.

Prior to this report, ergosterol had not been studied in the context of hematopoiesis. Although other vitamin D family members have been shown to have cell growth-promoting effects on the hematopoietic system and have been specifically utilized in the management of anemia (Christakos et al., 2013; Erturk et al., 2002; Hall and Juckett, 2013; Hewison et al., 2001). In addition, Cortes et al. (2016) have recently shown that vitamin D_3 has HSPC growth-promoting effects in embryonic zebrafish as well as in human umbilical cord blood. Furthermore, ergosterol may also have cytoprotective effects, as rats that receive ergosterol prior to carbon-tetrachloride-induced liver injury have a significant reduction in liver injury, inflammation, and fibrosis (Peng et al., 2014). These data are consistent with our finding that cells exposed to ergosterol have improved viability.

There are increasing data that vitamin D plays a positive role in HCT (Hall and Juckett, 2013). Hansson et al. (2014) recently measured vitamin D levels (total vitamin D including D_2 and D_3) in children prior to HCT. They found that children who were vitamin D-sufficient pre-HCT had more robust neutrophil engraftment at day 30 post-HCT (the first time point measured) and lower rates of hematopoietic cell rejection. Vitamin D-sufficient children with malignancy also had improved overall survival (87% versus 50%, $p = 0.01$). Other groups have shown that severe vitamin D deficiency at HCT was associated with reduced survival after transplant in pediatric patients (Wallace et al., 2015). These reports suggest that vitamin D positively affects engraftment and overall HCT outcome. The mechanisms for the enhancement of engraftment were not demonstrated, but our data suggest that perhaps vitamin D family members can increase CXCR4 expression, one of the key mediators of homing after transplant.

In this study, we demonstrated BLI to be a useful tool to non-invasively track transplanted hematopoietic cells in the zebrafish, allowing the homing/engraftment process to be observed in a living adult recipient. The quantified luminescent signals were consistent and corresponded well with the number of cells engrafting. Our longitudinal analysis demonstrated the kinetics of donor WKM cells showing a high level of engraftment by short-term progenitor cells, and lower, stable level of engraftment by more rare long-term repopulating stem cells. Using BLI, we were able to perform a chemical screen of compounds to find those that enhance cellular homing. We found that ergosterol, a phytosterol and vitamin D_2 precursor, improves homing of hematopoietic cells in zebrafish and mouse models. The mechanism of action is incompletely understood, although CXCR4 upregulation plays a role and likely involves pleiotropic effects on cell expansion and survival.

EXPERIMENTAL PROCEDURES

Fish Husbandry

Zebrafish were bred and maintained at the University of Minnesota Zebrafish Core Facility according to standard guidelines (Westerfield, 1993) and with the approval of the Institutional Animal Care and Use Committee, University of Minnesota. The following lines were used: Segrest wild-type, *ubi:luc*, and *ubi:luc x h2afv:gfp*.

Creation of *ubi:luc* Transgenic Fish

The *ubiquitin* promoter was cloned upstream of *luciferase* on a Tol2-based backbone containing the *myosin light-chain 2* promoter driving the *green fluorescent protein* gene. This construct was injected along with Tol2 transposase mRNA into early

zebrafish embryos (Davidson et al., 2003; Mosimann et al., 2011). Embryos were screened for GFP-positive hearts, raised to adulthood, and out-crossed to establish independent lines. Independent lines from F2 generation fish were generated from separate F1 parents to reduce variability in luciferase expression.

WKM Cells Isolation

Fish were euthanized by immersion in ice water until the heart stopped beating. The aorta was flushed with PBS to remove the peripheral blood. WKM was then dissected, triturated using a P1000 pipette, filtered through a 40-μm filter, and centrifuged at 2,000 × *g* for 6 min. The supernatant was removed and WKM cells were suspended in PBS for use.

Zebrafish Hematopoietic Cell Transplantation

Irradiation was given using an X-Rad 320 irradiator (Precision X-Ray). During irradiation, fish were put in a large Petri dish containing fish water. The irradiation dose was 20 Gy at a rate of 2.7 Gy/min. Transplantation was performed 2 days after irradiation, at the time of hematopoietic nadir. Recipient fish were anesthetized with 0.01% tricaine methanesulfonate and placed on a wet sponge. Donor cells were injected via an intracardiac route in a 5 μL volume using a 30-gauge Hamilton syringe. Recipient fish were transplanted with 50,000–500,000 cells (depending on the experiment) and with the compound or equal v/v vehicle.

Bioluminescence Imaging

For in vitro BLI, cells were suspended in PBS containing 150 μg/mL D-luciferin (Gold Biotechnology) and immediately imaged at 1- to 5-min exposure. For in vivo BLI in zebrafish embryos, embryos were placed in fish water containing 150 μg/mL D-luciferin. For in vivo BLI in adult zebrafish, fish were intraperitoneally injected with 5 μL of 15 mg/mL D-luciferin and imaged 10–15 min after injection. At the time of imaging, fish were anesthetized with 65 parts per million (ppm) oisoflurane and 65 ppm tricaine in hyper-oxygenated fish water. The hyper-oxygenated fish water was prepared by immersing oxygen bubbler in the fish water until the dissolved oxygen was higher than 20 mg/L. Optical images were acquired with a CCD camera (Xenogen IVIS50 system, Caliper Life Sciences) and analyzed with Living Image (Caliper Life Sciences) software. Images were taken at a 1-min exposure with CCD resolution set at 4–8 pixel binning. After imaging, fish were allowed to recover in hyper-oxygenated fish water. The region of interest was manually drawn during analysis. The average radiance (photons/s/cm^2/sr) or total flux (in photons/s) were acquired as measurements of the luminescent signal. We found no difference between using radiance or total flux values relative to control animals when determining changes in luminescence.

Immunofluorescence

WKM cells were harvested, dropped on to slides, and air dried. Cells were then fixed with cold 100% methanol for 5 min, permeabilized with 0.4% Triton X-100 in PBS for 10 min, and blocked with 1% BSA in PBS + 0.1% Tween 20 for 1 hr at room temperature. Cells were probed with mouse monoclonal anti-luciferase antibody (no. ab21176, Abcam) or mouse immunoglobulin G1 (IgG1) isotype control (no. 11711, Novus Biologicals) at a ratio of 1:100 overnight at 4°C, followed by donkey polyclonal anti-mouse IgG1-Cy3 (no. 715-165-150, Jackson ImmunoResearch) at 1:300 for 1 hr at room temperature. Nuclei were stained with DAPI.

dmPGE$_2$ Treatment and Chemical Screen

A total of 200,000 WKM cells was incubated with zebrafish medium containing 50 μM dmPGE$_2$ (Cayman Chemical) in DMSO for 2 hr on ice. DMSO was used as vehicle control. Cells were then washed twice with and suspended in PBS before delivery to recipient fish as described before. The chemical screen was performed using the NatProd Collection from MicroSource Discovery Systems. All chemicals were in DMSO at a concentration of 10 mM and diluted to 10 μM when mixed with donor WKM cells. Transplants were performed as stated above.

Murine Hematopoietic Cell Transplantation

Recipient C57bl/6NCr CD45.2 mice were subjected to 9 Gy of myeloablative radiation at a dose rate of 83 rad/min 24 hr prior to transplant. Donor marrow was prepared from B6.SJL-Ptprc^{a}Pepc^b/BoyCrl (CD45.1) mice at a concentration of 2.5 × 10^7 cells/mL in Hank's balanced salt solution. Ergosterol was dissolved in ethanol at a stock concentration of 5 mM and added to the cell suspension for injection at a final concentration of 50 μM. Cells (1 × 10^7) were delivered via tail vein injection in a volume of 0.2 mL to achieve a circulating concentration of 10 μM. Marrow was harvested from recipients 16 hr post-transplant. Mice were flushed with 10 mL PBS and femurs removed. Femurs were crushed by motor and pestle followed by incubation in Accutase (Sigma-Aldrich) at 37°C for 15 min while shaking to isolate hematopoietic cells. Cells were passed through a 40-μm filter and washed twice in PBS prior to flow cytometry. The following antibodies were used to determine donor LSK: AlexaFluor 647 anti-mouse CD45.1 (no. 110720, BioLegend), Pacific Blue anti-mouse CD45.2 (no. 109820, BioLegend), Lineage Cocktail-fluorescein isothiocyanate (no. 133302, BioLegend), anti-mouse Ly-6A/E (SCA-1) phycoerythrin (no. 12-5981-82, eBioScience), anti-mouse CD117 (KIT) allophycocyanin-e-Fluor 780 (no. 47-1172-82, eBioscience). CountBright Absolute Counting Beads (Life Technologies) were used to quantify absolute numbers of cells and propidium iodide (Sigma-Aldrich) was used to determine viability. Flow cytometry was performed using a BD FACSCanto (BD Biosciences) flow cytometer and FlowJo version 9.3.

Cell Migration, *Cxcr4* Expression, and In Vitro Hematopoietic Cell Expansion

See Supplemental Experimental Procedures.

Reporter Assays

See Supplemental Experimental Procedures.

AMD3100 Mobilization

Wild-type mice were given 0.2 mL of 50 μM ergosterol i.v. or equal v/v vehicle. Twenty-four hours later, mice received AMD3100 (3 mg/kg) via tail vein injection. One hour after AMD3100 administration, mice were killed via carbon dioxide asphyxiation and whole blood assessed for total cell counts on a Hemavet 950FS

Analyzer. To analyze CFU-C, whole blood was first lineage depleted using the EasySep Mouse Hematopoietic Progenitor Cell Isolation Kit according to the manufacturer's instructions (STEMCELL Technologies). To perform CFU-C assays, lineage-negative cells were cultured on MethoCult GF M3434 (STEMCELL Technologies) according to the manufacturer's instructions and readout after 14 days.

Radiation Recovery

Zebrafish received 25 Gy X-ray irradiation. Twenty-four hours later, 50 μM ergosterol (or equal v/v vehicle) was added to the water. WKM was harvested 14 days after radiation treatment and analyzed by flow cytometry using typical forward- and side-scatter gating for erythroid cells, myelomonocytes, precursors, and lymphocytes, as previously described (Traver et al., 2003). Cell viability was determined using propidium iodide exclusion.

Statistical Analysis

Quantitative data were presented as mean and SD as noted. Two-group analyses were performed using an unpaired Student's t test. Survival was analyzed using the Wilcoxon test. In vitro experiments were performed at least three times.

SUPPLEMENTAL INFORMATION

Supplemental Information includes Supplemental Experimental Procedures and three figures and can be found with this article online at http://dx.doi.org/10.1016/j.stemcr.2016.12.004.

AUTHOR CONTRIBUTIONS

Y.A. performed the majority of the experiments and wrote the first draft of the manuscript, A.K. assisted in transplant and in vitro experiment execution, B.R.B. edited the manuscript, J.T. edited the manuscript, A.L.B. and M.E.T. performed adoptive transfer experiments, T.C.L. oversaw the project, contributed to experimental design, and performed final manuscript editing and revisions.

ACKNOWLEDGMENTS

We gratefully thank the laboratory of Dr. Zon for sharing the *ubiquitin* promoter fragment. Research reported in this publication was supported by the National Heart, Lung and Blood Institute of the NIH under award number K08HL108998 (T.C.L.), ASH Junior Faculty Scholar Award (T.C.L.), the University of Minnesota Children's Discovery Fund (T.C.L.), a University of Minnesota Academic Health Center Seed Grant (T.C.L.), and a Minnesota Regenerative Medicine Grant (T.C.L.).

Received: December 14, 2015
Revised: December 1, 2016
Accepted: December 2, 2016
Published: December 29, 2016

REFERENCES

Bikle, D.D. (2014). Vitamin D metabolism, mechanism of action, and clinical applications. Chem. Biol. *21*, 319–329.

Biswas, P., Mengozzi, M., Mantelli, B., Delfanti, F., Brambilla, A., Vicenzi, E., and Poli, G. (1998). 1,25-Dihydroxyvitamin D3 upregulates functional CXCR4 human immunodeficiency virus type 1 coreceptors in U937 minus clones: NF-kappaB-independent enhancement of viral replication. J. Virol. *72*, 8380–8383.

Cao, Y.A., Wagers, A.J., Beilhack, A., Dusich, J., Bachmann, M.H., Negrin, R.S., Weissman, I.L., and Contag, C.H. (2004). Shifting foci of hematopoiesis during reconstitution from single stem cells. Proc. Natl. Acad. Sci. USA *101*, 221–226.

Carlberg, C. (2003). Current understanding of the function of the nuclear vitamin D receptor in response to its natural and synthetic ligands. Recent Results Cancer Res. *164*, 29–42.

Chen, C.H., Durand, E., Wang, J., Zon, L.I., and Poss, K.D. (2013). Zebraflash transgenic lines for in vivo bioluminescence imaging of stem cells and regeneration in adult zebrafish. Development *140*, 4988–4997.

Christakos, S., Hewison, M., Gardner, D.G., Wagner, C.L., Sergeev, I.N., Rutten, E., Pittas, A.G., Boland, R., Ferrucci, L., and Bikle, D.D. (2013). Vitamin D: beyond bone. Ann. N. Y. Acad. Sci. *1287*, 45–58.

Cortes, M., Chen, M.J., Stachura, D.L., Liu, S.Y., Kwan, W., Wright, F., Vo, L.T., Theodore, L.N., Esain, V., Frost, I.M., et al. (2016). Developmental vitamin D availability impacts hematopoietic stem cell production. Cell Rep. *17*, 458–468.

Davidson, A.E., Balciunas, D., Mohn, D., Shaffer, J., Hermanson, S., Sivasubbu, S., Cliff, M.P., Hackett, P.B., and Ekker, S.C. (2003). Efficient gene delivery and gene expression in zebrafish using the Sleeping Beauty transposon. Dev. Biol. *263*, 191–202.

de Jong, J.L., Burns, C.E., Chen, A.T., Pugach, E., Mayhall, E.A., Smith, A.C., Feldman, H.A., Zhou, Y., and Zon, L.I. (2011). Characterization of immune-matched hematopoietic transplantation in zebrafish. Blood *117*, 4234–4242.

Erturk, S., Kutlay, S., Karabulut, H.G., Keven, K., Nergizoglu, G., Ates, K., Bokesoy, I., and Duman, N. (2002). The impact of vitamin D receptor genotype on the management of anemia in hemodialysis patients. Am. J. Kidney Dis. *40*, 816–823.

Frisch, B.J., Porter, R.L., Gigliotti, B.J., Olm-Shipman, A.J., Weber, J.M., O'Keefe, R.J., Jordan, C.T., and Calvi, L.M. (2009). In vivo prostaglandin E2 treatment alters the bone marrow microenvironment and preferentially expands short-term hematopoietic stem cells. Blood *114*, 4054–4063.

Glass, T.J., Lund, T.C., Patrinostro, X., Tolar, J., Bowman, T.V., Zon, L.I., and Blazar, B.R. (2011). Stromal cell-derived factor-1 and hematopoietic cell homing in an adult zebrafish model of hematopoietic cell transplantation. Blood *118*, 766–774.

Glass, T.J., Hui, S.K., Blazar, B.R., and Lund, T.C. (2013). Effect of radiation dose-rate on hematopoietic cell engraftment in adult zebrafish. PLoS One *8*, e73745.

Hall, A.C., and Juckett, M.B. (2013). The role of vitamin D in hematologic disease and stem cell transplantation. Nutrients *5*, 2206–2221.

Hansson, M.E., Norlin, A.C., Omazic, B., Wikstrom, A.C., Bergman, P., Winiarski, J., Remberger, M., and Sundin, M. (2014). Vitamin D levels affect outcome in pediatric hematopoietic stem cell transplantation. Biol. Blood Marrow Transplant *20*, 1537–1543.

Hewison, M., Gacad, M.A., Lemire, J., and Adams, J.S. (2001). Vitamin D as a cytokine and hematopoetic factor. Rev. Endocr. Metab. Disord. *2*, 217–227.

Hiraguchi, Y., Tanida, H., Sugimoto, M., Hosoki, K., Nagao, M., Tokuda, R., and Fujisawa, T. (2012). 1,25-Dihydroxyvitamin D3 upregulates functional C-x-C chemokine receptor type 4 expression in human eosinophils. Int. Arch. Allergy Immunol. *158* (*Suppl 1*), 51–57.

Hoggatt, J., Singh, P., Sampath, J., and Pelus, L.M. (2009). Prostaglandin E2 enhances hematopoietic stem cell homing, survival, and proliferation. Blood *113*, 5444–5455.

Hollis, B.W. (1984). Comparison of equilibrium and disequilibrium assay conditions for ergocalciferol, cholecalciferol and their major metabolites. J. Steroid Biochem. *21*, 81–86.

Houghton, L.A., and Vieth, R. (2006). The case against ergocalciferol (vitamin D2) as a vitamin supplement. Am. J. Clin. Nutr. *84*, 694–697.

Lin, Y., Molter, J., Lee, Z., and Gerson, S.L. (2008). Bioluminescence imaging of hematopoietic stem cell repopulation in murine models. Methods Mol. Biol. *430*, 295–306.

Mosimann, C., Kaufman, C.K., Li, P., Pugach, E.K., Tamplin, O.J., and Zon, L.I. (2011). Ubiquitous transgene expression and Cre-based recombination driven by the ubiquitin promoter in zebrafish. Development *138*, 169–177.

North, T.E., Goessling, W., Walkley, C.R., Lengerke, C., Kopani, K.R., Lord, A.M., Weber, G.J., Bowman, T.V., Jang, I.H., Grosser, T., et al. (2007). Prostaglandin E2 regulates vertebrate haematopoietic stem cell homeostasis. Nature *447*, 1007–1011.

Pauls, S., Geldmacher-Voss, B., and Campos-Ortega, J.A. (2001). A zebrafish histone variant H2A.F/Z and a transgenic H2A.F/Z: GFP fusion protein for in vivo studies of embryonic development. Dev. Genes Evol. *211*, 603–610.

Peled, A., Petit, I., Kollet, O., Magid, M., Ponomaryov, T., Byk, T., Nagler, A., Ben-Hur, H., Many, A., Shultz, L., et al. (1999). Dependence of human stem cell engraftment and repopulation of NOD/SCID mice on CXCR4. Science *283*, 845–848.

Peng, Y., Tao, Y., Wang, Q., Shen, L., Yang, T., Liu, Z., and Liu, C. (2014). Ergosterol is the active compound of cultured mycelium cordyceps sinensis on antiliver fibrosis. Evid. Based. Complement. Altern. Med. *2014*, 537234.

Porter, R.L., Georger, M.A., Bromberg, O., McGrath, K.E., Frisch, B.J., Becker, M.W., and Calvi, L.M. (2013). Prostaglandin E2 increases hematopoietic stem cell survival and accelerates hematopoietic recovery after radiation injury. Stem Cells *31*, 372–383.

Ramirez, P., Rettig, M.P., Uy, G.L., Deych, E., Holt, M.S., Ritchey, J.K., and DiPersio, J.F. (2009). BIO5192, a small molecule inhibitor of VLA-4, mobilizes hematopoietic stem and progenitor cells. Blood *114*, 1340–1343.

Salcedo, R., Zhang, X., Young, H.A., Michael, N., Wasserman, K., Ma, W.H., Martins-Green, M., Murphy, W.J., and Oppenheim, J.J. (2003). Angiogenic effects of prostaglandin E2 are mediated by up-regulation of CXCR4 on human microvascular endothelial cells. Blood *102*, 1966–1977.

Savli, H., Aalto, Y., Nagy, B., Knuutila, S., and Pakkala, S. (2002). Gene expression analysis of 1,25(OH)2D3-dependent differentiation of HL-60 cells: a cDNA array study. Br. J. Haematol. *118*, 1065–1070.

Traver, D., Paw, B.H., Poss, K.D., Penberthy, W.T., Lin, S., and Zon, L.I. (2003). Transplantation and in vivo imaging of multilineage engraftment in zebrafish bloodless mutants. Nat. Immunol. *4*, 1238–1246.

Traver, D., Winzeler, A., Stern, H.M., Mayhall, E.A., Langenau, D.M., Kutok, J.L., Look, A.T., and Zon, L.I. (2004). Effects of lethal irradiation in zebrafish and rescue by hematopoietic cell transplantation. Blood *104*, 1298.

Wallace, G., Jodele, S., Howell, J., Myers, K.C., Teusink, A., Zhao, X., Setchell, K., Holtzapfel, C., Lane, A., Taggart, C., et al. (2015). Vitamin D deficiency and survival in children after hematopoietic stem cell transplant. Biol. Blood Marrow Transplant *21*, 1627–1631.

Wang, X., Rosol, M., Ge, S., Peterson, D., McNamara, G., Pollack, H., Kohn, D.B., Nelson, M.D., and Crooks, G.M. (2003). Dynamic tracking of human hematopoietic stem cell engraftment using in vivo bioluminescence imaging. Blood *102*, 3478–3482.

Westerfield, M. (1993). The Zebrafish Book: A Guide for the Laboratory Use of Zebrafish (*Brachydanio rerio*) (University of Oregon Press).

White, R.M., Sessa, A., Burke, C., Bowman, T., LeBlanc, J., Ceol, C., Bourque, C., Dovey, M., Goessling, W., Burns, C.E., et al. (2008). Transparent adult zebrafish as a tool for in vivo transplantation analysis. Cell Stem Cell *2*, 183–189.